

Collective-pinning theory and the observed vortex dynamics in $R\text{Ba}_2\text{Cu}_3\text{O}_{7-\delta}$ crystals

G. K. Perkins and A. D. Caplin

Centre for High Temperature Superconductivity, Blackett Laboratory, Imperial College, London SW7 2BZ, United Kingdom

(Received 6 May 1996; revised manuscript received 26 June 1996)

We establish a framework for the analysis of magnetization data on high-temperature superconductor crystals that allows direct comparison with vortex-pinning theory. When the magnetization loops exhibit scaling behavior, as they do over a large part of the B - T plane for $R\text{Ba}_2\text{Cu}_3\text{O}_{7-\delta}$ crystals, the effective pinning energy U_{eff} has to contain power-law field dependences for the characteristic energy and current scales U_0 and J_0 ; these power-law exponents can be obtained directly from the data. Many regimes of collective-pinning (CP) theory do predict such power laws, but none yield exponents in agreement with those that are measured. The discrepancy appears to arise because U_0 is observed to decrease with B , in contrast to the CP predictions. [S0163-1829(96)01441-5]

I. INTRODUCTION

Attempts to understand the dissipation mechanism in high-temperature superconductors (HTSC's) have led to a large body of work, both experimental and theoretical, in recent years. Most assessments of the validity of current theories by comparison with experimental data result in ambiguity, because of the large number of free parameters involved in the fitting procedure. Consequently it is unclear which, if any, of these theories¹ is appropriate. Essentially, a successful theory must give an accurate description of the macroscopic electrodynamics, and its field and temperature dependences, because it is these that are ultimately determined by the microscopic vortex dynamics.

In this paper we extend the analysis of magnetisation loop scaling described in Ref. 2 and compare in detail the experimental results for $R\text{Ba}_2\text{Cu}_3\text{O}_{7-\delta}$ with a range of current theoretical predictions.

II. MEASUREMENT OF THE E - J - B SURFACE

The measured electrodynamics (i.e., the relation between the electric field E , the current density J , and the magnetic induction B), and so also the microscopic behavior, may be summarized as an E - J - B surface (experimentally, care must be taken to ensure that bulk effects are dominant, so that surface and geometric artefacts do not distort the data);³ this may then be compared with the predictions of theory. At a single temperature, if one considers the geometric relation

$$\left(\frac{\partial \ln E}{\partial \ln J}\right)_B \left(\frac{\partial \ln J}{\partial \ln B}\right)_E \left(\frac{\partial \ln B}{\partial \ln E}\right)_J = -1, \quad (1)$$

it is clear that knowledge of just two of the three logarithmic differentials contains all the relevant information about the surface, and such relationships therefore reflect the underlying physics.

In magnetization experiments $(\partial \ln J / \partial \ln E)_{B,T}$ and $(\partial \ln J / \partial \ln B)_{E,T}$ are measured directly (usually with B as the intrinsic parameter) and are equivalent to the quantities S (the normalized creep rate) and χ_{\ln} (the logarithmic susceptibility), respectively. Because of their fundamental signifi-

cance, it is natural to plot χ_{\ln} versus S in order to analyze the vortex behavior. The experiments show that both χ_{\ln} and S vary smoothly with T , but as a function of B may display maxima and minima.

III. INTERPRETATION OF χ_{\ln} AND S IN TERMS OF THERMALLY ACTIVATED CREEP

For thermally activated vortex motion the E - J - B - T relation is

$$E = B \nu d \exp\left[-\frac{U_{\text{eff}}(J,B,T)}{kT}\right] \quad (2)$$

where ν is an attempt frequency, d is the hop distance, and $U_{\text{eff}}(J,B,T)$, the effective energy barrier for thermally activated jumps, contains the vortex dynamics.

Theoretical analyses tend to focus on the form of U_{eff} as a function of J , but as we have pointed out previously,³ in an experiment at fixed B and T , the accessible range of J is extremely narrow, typically much less than a factor of 2. Consequently, it is usually difficult to distinguish between different predicted forms of $U_{\text{eff}}(J)$.

An additional (but reasonable) assumption is that $U_{\text{eff}}(J,B,T)$ may be separated as⁴

$$U_{\text{eff}}(J,B,T) = U_0(B,T) V[J/J_0(B,T)] \quad (3)$$

where the parameters $U_0(B,T)$ and $J_0(B,T)$ represent characteristic energy and current scales, and $V(J/J_0)$ describes the functional dependence of U_{eff} on J .

Combining Eqs. (2) and (3) gives a general relationship between the macroscopic electrodynamic variables (E , J , B , and T) and the pinning functions U_0 , J_0 , and V :

$$U_0(B,T) V[J/J_0(B,T)] = kTC, \quad (4)$$

where $C = \ln[B \nu d / E]$ and for usual experimental conditions is almost constant (typically ≈ 20 for a R -Ba-Cu-O crystal).^{4,5,2}

One can now proceed to analyze the behavior of χ_{\ln} and S within this framework. Differentiating Eq. (4) gives for χ_{\ln} and S :

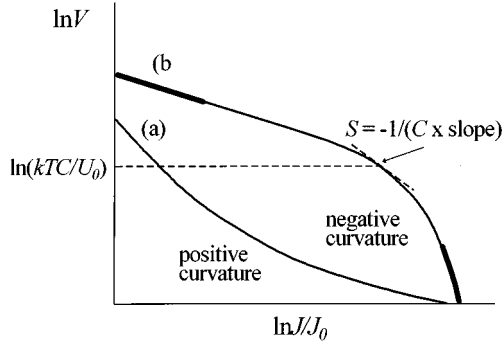


FIG. 1. Schematic plot of the function $V(J/J_0)$ that controls the dependence of U_{eff} on J . Curve (a) has positive logarithmic curvature whilst curve (b) has zero curvature at low J (shown bold), and negative curvature as it approaches the high J limit (also bold). The experimental conditions set the value of V , which is equal to kTC/U_0 , and S is determined by the logarithmic slope at this point. For positive (negative) logarithmic curvature of the function $V(J/J_0)$, S is an increasing (decreasing) function of kTC/U_0 .

$$\chi_{\text{ln}} = \left[\frac{\partial \ln J_0(B, T)}{\partial \ln B} \right]_{E, T} + \frac{1}{V'_{\text{ln}}} \left\{ \frac{1}{C} - \left[\frac{\partial \ln U_0(B, T)}{\partial \ln B} \right]_{E, T} \right\} \quad (5)$$

and

$$S = \frac{-1}{CV'_{\text{ln}}}, \quad (6)$$

where V'_{ln} is the logarithmic differential of $V(J/J_0)$ with respect to J/J_0 . Equation (6) shows that S is controlled primarily by V'_{ln} , and because $V = kTC/U_0$ [Eq. (4)], S is essentially a function (related to V) of T/U_0 , as illustrated in Fig. 1. For example, at fixed T and with positive logarithmic curvature for V , and with U_0 increasing with B , S increases with B . Reversing either condition changes the sense in which S depends on B . Experimentally both S increasing and decreasing with B are seen, as in Fig. 2(a).

The behavior of χ_{ln} is more complicated because it includes the field dependences of J_0 and U_0 . However, if these field dependences are power laws, so that the differentials in Eq. (5) are constant, χ_{ln} is controlled solely by V'_{ln} and hence behaves in a similar fashion to S . This situation is often found experimentally in R -Ba-Cu-O crystals, and has important consequences that are discussed below.

IV. INFLUENCE OF SCALING ON THE χ_{ln} VERSUS S RELATIONSHIP

It has often been observed that, over large regions of the B - T plane, the magnetization loops of R -Ba-Cu-O, crystals retain their shape with changing temperature (and also with changing electric field). This scaling behavior represents a special case for the χ_{ln} vs S relationship.²

A. Scaling in general

In the general case, scaling of the magnetization loops can be expressed as

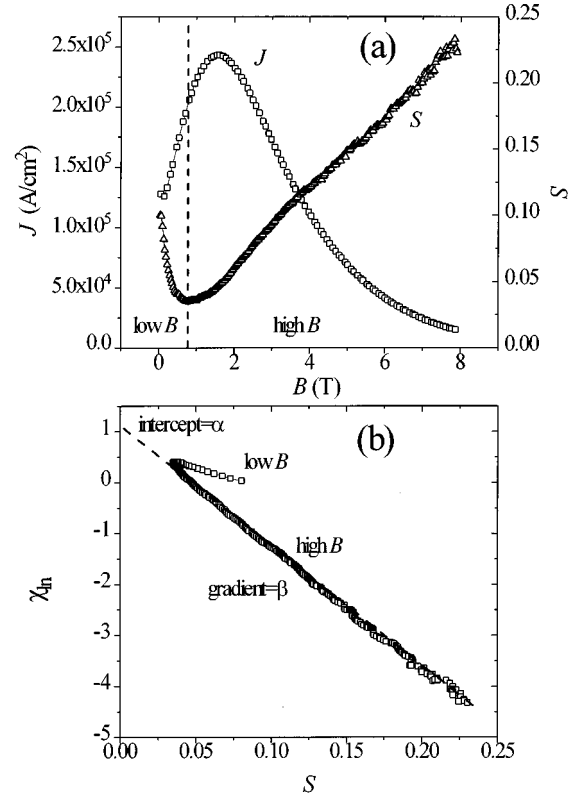


FIG. 2. (a) The magnetically measured current density $J(B)$ and creep rate $S(B)$ for a $\text{TmBa}_2\text{Cu}_3\text{O}_{6.8}$ crystal at 50 K (Ref. 8). (b) The same data in the form of logarithmic susceptibility χ_{ln} plotted against the normalized creep rate S , with B as the implicit variable. The present analysis focuses on the high-field regime, above the minimum in S .

$$\frac{J}{J_{\text{char}}(E, T)} = \varphi \left[\frac{B}{B_{\text{char}}(E, T)} \right], \quad (7)$$

where $J_{\text{char}}(E, T)$ and $B_{\text{char}}(E, T)$ refer to characteristic scales of J and B . Bearing in mind that in logarithmic coordinates, the scaling is associated with simple translations, it can be seen that any contour of constant χ_{ln} on the E - J - B surface may be utilized as the fiducial feature. For example, the well-known ‘fishtail’ peak in R -Ba-Cu-O (Refs. 6 and 7) is often used to define the coordinates (J_{char} , B_{char}), and simply reflects the locus on the E - J - B surface where $\chi_{\text{ln}} = 0$; in principle, any value of χ_{ln} will do.

It was discussed in Ref. 2 that Eq. (7) implies two separate types of scaling: scaling across a range of temperature but at constant electric field (temperature scaling) and scaling across a range of electric fields at a fixed temperature. The latter (electric-field scaling) is the focus of this paper and, as shown in Ref. 2, is equivalent to a linear relation between χ_{ln} and S :

$$\chi_{\text{ln}} = \alpha + \beta S, \quad (8)$$

where α and β are independent of B . Thus, when electric-field scaling is present, the isothermal behavior can be characterized by two independent dimensionless parameters, α and β , and we therefore expect these to reflect fundamental aspects of the pinning mechanism.

Although HTSC crystals do often display both temperature- and electric-field scaling, there is no fundamental reason for one to require the other. The test for the presence of electric-field scaling is the existence of a significant linear relationship between χ_{ln} and S , for example as in Fig 2.

B. Interpretation of scaling in terms of thermally activated creep

The scaling behavior discussed previously can be analyzed within the framework of thermally activated vortex motion outlined in Sec. III. Such an analysis was described first in Ref. 2, and is taken further in Appendix A. The key results are summarized below.

(1) The scaling condition [Eq. (7)] when combined with Eq. (4) requires both separability and power laws with respect to field for both $U_0(B,T)$ and $J_0(B,T)$

$$J_0(B,T) = \Lambda(T)B^m, \quad (9)$$

$$U_0(B,T) = \Psi(T)B^n, \quad (10)$$

where we have introduced the temperature dependences $\Lambda(T)$ and $\Psi(T)$ and the power-law exponents m and n .

(2) The parameters m , n , and functions $\Psi(T)$, $\Lambda(T)$, and $V(J)$ can all be found directly from the experimental data by utilizing the χ_{ln} versus S plots [Eq. (8)] and the relationships

$$m = \alpha, \quad (11)$$

$$n = (\beta + 1)/C, \quad (12)$$

$$\Psi(T) \propto CTB_{\text{char}}^{-n}(E,T), \quad (13)$$

$$\Lambda(T) \propto \frac{J_{\text{char}}(E,T)}{B_{\text{char}}^m(E,T)}, \quad (14)$$

$$V \left[\frac{J(B)}{\Lambda(T)B^m} \right] \propto \frac{B^{-n}T}{\Psi(T)}. \quad (15)$$

V. COMPARISON BETWEEN EXPERIMENT AND COLLECTIVE-PINNING THEORY

Figure 2(a) shows the directly measured current density $J(B)$ and the corresponding creep rate $S(B)$ for a $\text{TmBa}_2\text{Cu}_3\text{O}_{6.8}$ crystal at 50 K; qualitatively similar behavior has been found in a large number of $R\text{-Ba-Cu-O}$ crystals over wide ranges of field and temperature. Also, there are systematic trends as the oxygen content is reduced, with a consequent increase in anisotropy.⁸

The data are replotted in Fig. 2(b) as χ_{ln} versus S with B as the intrinsic variable, as suggested by Eq. (8). There are two linear segments on this plot, relating to the scaling behavior discussed in Sec. IV A. The short segment represents the low-field behavior and the long segment the high-field behavior; in all the $R\text{-Ba-Cu-O}$ crystals that have been studied, the largest area of the $B\text{-}T$ plane is associated with the latter. For the present, the former will not be discussed.

In the high-field segment, experiments reveal typical values for α and β of 1 and -20 respectively. Consequently from Eqs. (11) and (12) the experimental results on $R\text{-Ba-}$

Cu-O indicate that $m \approx 1$ and $n \approx -1$; these values are found to be almost independent of individual sample peculiarities, oxygen stoichiometry, and temperature.⁸ The data indicate also weak temperature dependences for both Ψ and Λ and an approximate logarithmic form for V ,⁸ but these aspects will not be discussed here.

We now focus on the observed power-law field dependences of $J_0(B,T)$ and $U_0(B,T)$, and the specific values of the exponents m and n . It is these that are intrinsic to the pinning mechanism that dominates in $R\text{-Ba-Cu-O}$, and which should be compared to relevant theory. The collective-pinning^{9,1} (CP) model is the most appropriate starting point for such a comparison.

The approach of CP is to describe the vortex lattice (VL) as an elastic continuum which interacts with a weak-random-disorder potential (we will not discuss other types of disorder here). In this situation the Abrikosov vortex lattice is replaced by a ‘‘glassy’’ array in which the vortex positions are correlated only within a ‘‘vortex bundle’’ of volume V_C . It is these bundles or groups of bundles (superbundles) that move by thermally activated jumps. A full treatment leads to several different predicted regimes of behavior (single vortex, small bundle, etc.), with a number of limiting cases for each (for example, ‘‘small driving force’’ for $J \ll J_C$, and ‘‘near criticality’’ for $J \sim J_C$). However, in each of these regimes the predicted dependences of $U_{\text{eff}}(J,B,T)$ can be expressed in the form of Eq. (3) but with distinct dependences for $U_0(B,T)$, $J_0(B,T)$, and $V(J/J_0)$.

We start with the predicted behavior of the function $V(J/J_0)$. For small driving forces $J \ll J_C$ collective pinning predicts

$$V \left(\frac{J}{J_0} \right) = \left(\frac{J}{J_0} \right)^{-\mu}, \quad (16)$$

where μ is positive. Near criticality, with $J \sim J_C$, the result is

$$V \left(\frac{J}{J_C} \right) = \left[1 - \frac{J}{J_c(B,T)} \right]^\alpha, \quad (17)$$

where α is positive.

Assuming that there is a smooth monotonic crossover between the two forms, the functional form of V may be represented schematically by curve (b) in Fig. 1. Because V'_{ln} is constant ($-\mu$) for low J , the logarithmic curvature of V is zero in this regime. For high J , the (logarithmic) gradient of V becomes increasingly negative, with $-V'_{\text{ln}} > \mu$. From Eq. (6) it follows that $S \leq 1/\mu C$. Consider also what happens as an isothermal magnetisation loop is traced out: the experimental conditions fix kTC , but the magnitude of $U_0(B,T)$ will decrease with increasing B [Eq. (10) with $n \approx -1$]; consequently, the ‘‘operating point’’ indicated in Fig. 1 moves to a larger value of V with less negative slope, and S increases.

This information, together with the field dependences of J_0 and U_0 , may be used to generate the χ_{ln} versus S relationships that should be seen in different CP regimes. In many cases power-law field dependences, as in Eqs. (9) and (10), are predicted by CP (Appendix B) and we need consider only these, because anything else is inconsistent with

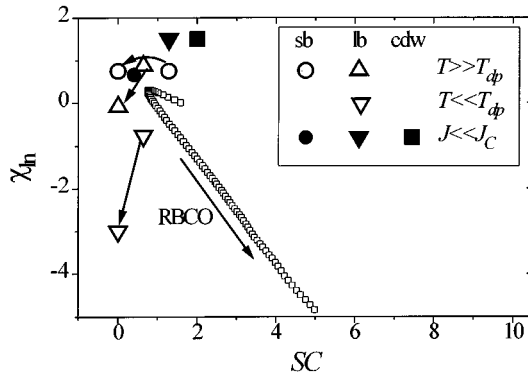


FIG. 3. Predicted behavior of χ_{\ln} against SC for various collective-pinning regimes, calculated with $C=20$. Where χ_{\ln} and S are predicted to vary with B , an arrow indicates the direction corresponding to increasing B . Data for a $\text{TmBa}_2\text{Cu}_3\text{O}_{6.8}$ crystal at 50 K are shown also.

the scaling behavior that is observed to dominate the B - T plane in R -Ba-Cu-O crystals. As we noted in Sec. IV, such power laws yield linear plots of χ_{\ln} against S ; in Fig. 3 these are compared with typical data.

There is clearly a major discrepancy between theory and experiment. All the CP regimes predict S to be either decreasing or constant with increasing magnetic field; that S is measured to *increase* with increasing B is incontrovertibly at odds with theory.

Underlying the CP prediction for the sign of the dependence of S on B is that usually U_0 is expected to increase with B (because of a stiffening of the vortex lattice as it becomes denser, leading to larger correlated bundles), resulting in positive slope for the χ_{\ln} versus S plots. The data, on the other hand, have negative slope, showing that U_0 *decreases* with increasing B .

The situation may be clarified by plotting the power-law exponents m and n for the different CP regimes (Fig. 4). It can be seen that within the population of different regimes, m and n tend to anticorrelate. This can be understood by considering that the pinning energy of a bundle is usually an increasing function of the correlation volume V_C , but the

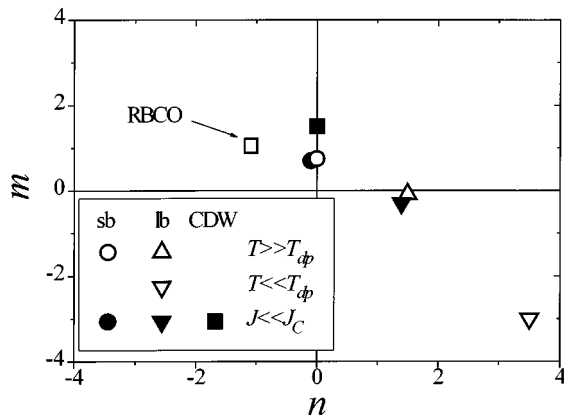


FIG. 4. The predicted values of the exponents m and n for the power-law field dependence of J_0 and U_0 corresponding to each of the regimes in Fig. 3. Data for $\text{TmBa}_2\text{Cu}_3\text{O}_{6.8}$ crystals are shown also.

pinning force is a decreasing function of V_C . In these terms, the location of the R -Ba-Cu-O data in the plot of Fig. 4, with U_0 decreasing with B , suggests that the VL softens with increasing B faster than any of the CP regimes that have been considered so far. Alternatively one could question the appropriateness of the elastic description of the VL. In which case a model describing some kind of *plastic* vortex motion might be more successful.

Note that we have made a direct comparison to theory only in certain limiting cases where power laws for $U_0(B)$ and $J_0(B)$ are predicted. Between these limiting cases more complex non-power-law behavior is predicted that is inconsistent with the observed scaling of the magnetization loops. Furthermore the general argument that U_0 should usually grow with increasing B still applies between these limits, and therefore the theory remains in conflict with the observation that U_0 decreases with B over a wide range of B and T .

VI. CONCLUSIONS

The most direct way to assess the physical behavior associated with magnetisation data on vortex pinning in HTSC crystals is to examine the logarithmic susceptibility χ_{\ln} as a function of the normalized creep rate S . A detailed comparison of the predictions in a number of different regimes of collective-pinning theory shows that none of them account satisfactorily for the data obtained on R -Ba-Cu-O crystals; the key discrepancy appears to be in the dependence of the characteristic energy scale $U_0(B, T)$ on B . The discrepancy could lie in the field dependence of C_{66} , which would need to soften monotonically over a wide field range in order to explain the results. The inclusion of the role of vortex lattice defects, or perhaps a consideration of the effects of vortex lattice melting may lead to such effects. On the other hand, it may be that the elastic response described by CP is not appropriate in these samples within the B - T window under consideration. Whatever the case, a successful theory of vortex motion in R -Ba-Cu-O must be consistent with the electric-field scaling behavior in $J(B)$, equivalent to a linear relationship between χ_{\ln} and S , which is observed to dominate a large part of the B - T plane. Also, it must yield the correct values of the power-law exponents for the observed field dependences of $U_0(B, T)$ and $J_0(B, T)$.

ACKNOWLEDGMENTS

We thank L. F. Cohen, A. A. Zhukov, J. Totty, and V. M. Vinokur for discussions that have helped to clarify issues raised in this work. This program is supported by the UK Engineering and Physical Sciences Research Council, Grant No. GR/K60916.

APPENDIX A: SCALING AND POWER LAWS

In Ref. 2 it was shown that the electric-field scaling of $J(B, T, E)$ is compatible with Eq. (4) only if the following hold:

$$\frac{\partial}{\partial \ln B} \left(\frac{\partial \ln J_0}{\partial \ln B} \right)_T = 0, \quad (\text{A1})$$

$$\frac{\partial}{\partial \ln B} \left(\frac{\partial \ln U_0}{\partial \ln B} \right)_T = 0, \quad (\text{A2})$$

so that J_0 and U_0 must have power dependences with respect to B . If temperature scaling is present as well then the following must also hold:²

$$\frac{\partial}{\partial \ln B} \left(\frac{\partial \ln J_0}{\partial \ln T} \right)_B = 0, \quad (\text{A3})$$

$$\frac{\partial}{\partial \ln B} \left(\frac{\partial \ln U_0}{\partial \ln T} \right)_B = 0. \quad (\text{A4})$$

Bearing in mind the commutative property of partial derivatives one can see that Eqs. (A3) and (A4) *require* $(\partial \ln J_0 / \partial \ln B)_T$ and $(\partial \ln U_0 / \partial \ln B)_T$ (i.e., the exponents m and n) to be temperature independent. This implies separability and power laws (in B) for $U_0(B, T)$ and $J_0(B, T)$:

$$J_0(B, T) = \Lambda(T) B^m, \quad (\text{A5})$$

$$U_0(B, T) = \Psi(T) B^n. \quad (\text{A6})$$

Substitution of Eq. (5) into Eq. (6) then leads to the following relation between $\chi_{\ln}(B)$ and $S(B)$:

$$\chi_{\ln} = m + (nC - 1)S. \quad (\text{A7})$$

Comparison of Eq. (A7) with Eq. (8) shows that

$$\alpha = m, \quad (\text{A8})$$

$$\beta = nC - 1, \quad (\text{A9})$$

implying that α and β (i.e., the measured intercept and gradient of the χ_{\ln} vs S plot) are temperature independent (as is often observed).

Note that although, in principle, it is possible to have electric-field scaling without temperature scaling (or vice versa), within the interpretation outlined here this would require the exponents n and m to be temperature dependent. In the context of CP theory this is rather unphysical. However, a different model for the underlying physics may well lead to different implications of the electric-field scaling that we observe.

The functions $\Psi(T)$ and $\Lambda(T)$ can be determined more directly than suggested in Ref. 2, by using Eq. (5) and substituting for $J_0(B, T)$ and $U_0(B, T)$ with Eqs. (A5) and (A6):

$$\chi_{\ln} = m + \frac{(C^{-1} - n)}{V'_{\ln}}. \quad (\text{A10})$$

Bearing in mind that by definition χ_{\ln} is constant for all $B = B_{\text{char}}$ (Sec. IV A), it follows from Eq. (4) that

$$\left[\frac{kTC}{\Psi(T) B_{\text{char}}^n(E, T)} \right] = \text{const}, \quad (\text{A11})$$

assuming that $(C^{-1} - n)$ is constant (which is an accurate approximation when $-n \gg C^{-1}$, typically $n \sim -1$ and $C^{-1} \sim 0.05$ so that small variations in C have virtually no effect). Hence

TABLE I. (a) Predicted values within collective-pinning theory for the exponents n and m at large driving forces ($J \sim J_C$) in the high-temperature limit $T \gg T_{\text{dp}}$. (b) Predicted values within collective-pinning theory for the exponents n and m at large driving forces ($J \sim J_C$) in the low-temperature limit $T \ll T_{\text{dp}}$. The small bundle case produces non-power-law behavior.

Parameter	Single vortex	Small bundle	Large bundle
		(a)	
n	0	0	3/2
m	0	3/4	-1/12
		(b)	
n	0		7/2
m	0		-3

$$\Psi(T) \propto CT B_{\text{char}}^{-n}(E, T). \quad (\text{A12})$$

Note that because Ψ is independent of E , the weak electric-field dependences of both C and B_{char}^{-n} cancel out. Also, by similar arguments, combining Eqs. (9) and (4) leads to

$$\frac{J_{\text{char}}(E, T)}{\Lambda(T) B_{\text{char}}^m(E, T)} = \text{const}, \quad (\text{A13})$$

hence

$$\Lambda(T) \propto \frac{J_{\text{char}}(E, T)}{B_{\text{char}}^m(E, T)}. \quad (\text{A14})$$

Again the weak electric-field dependences of J_{char} and B_{char}^m cancel out.

APPENDIX B: POWER-LAW EXPONENTS IN CP THEORY

Here we extract some of the predicted dependences of U_0 and J_0 on B given by CP (for three-dimensional behavior). These dependences are obtained from Ref. 1. We have not included regimes where $U_0(B)$ and $J_0(B)$ are not power laws, for these would be inconsistent with the observed scaling behavior of $J(B)$; nonlocal effects within the VL may give rise to such regimes.

First we cover the regime where the driving force J is close to criticality, $J \sim J_C$. Here $U_{\text{eff}}(J, B, T)$ is predicted to be of the form

$$U_{\text{eff}}(J, B, T) = U_C(B, T) \left[1 - \frac{J}{J_C(B, T)} \right]^\alpha, \quad (\text{B1})$$

where U_C and J_C are the pinning energy and critical current density, respectively. Power laws for $J_0(B)$ and $U_0(B)$, i.e., $J_C(B) \propto B^m$ and $U_C(B) \propto B^n$, are predicted in two limiting cases, depending on whether the thermal-fluctuations are greater or smaller than the superconducting coherence length, corresponding to $T > T_{\text{dp}}$ and $T < T_{\text{dp}}$, respectively, where T_{dp} is the thermal softening or depinning temperature. Note that between these limits, more complex non-power-law behaviors are predicted which cannot be in agreement with experiment because they are inconsistent with the observed scaling behavior of the $M(H)$ loops. The exponents m and n for the two limiting cases are shown in Table I.

For small driving forces $J \ll J_C$, the functional forms of $U_{\text{eff}}(J, B, T)$ are predicted to be

$$U_{\text{eff}}(J, B, T) = U_0(B, T) \left[\frac{J}{J_0(B, T)} \right]^{-\mu}, \quad (\text{B2})$$

where $U_0(B)$ and $J_0(B)$ are again power laws. Because here $V(J/J_0)$ is also a power law (with exponent $-\mu$), Eqs. (5) and (6) can be written as

$$\chi_{\text{ln}} = m + n/\mu \quad (\text{neglecting the } 1/C \text{ term}) \quad (\text{B3})$$

and

$$S = 1/\mu C, \quad (\text{B4})$$

hence both χ_{ln} and S are predicted to be field and temperature independent for small driving forces. The predicted values for m , n , and μ and the corresponding values for χ_{ln} and S [using Eqs. (B3) and (B4) and with $C=20$] are shown in Table II (these results do not include the effects of thermal fluctuations of the VL).

In this limit of low J , the theory gives for each regime just a single point on the χ_{ln} versus S plot of Fig. 3. The observed linear relation between χ_{ln} and S with B as an implicit variable demonstrates immediately that the theory is inappropriate.

TABLE II. Predicted values for the exponents n and m and μ at small driving forces ($J \ll J_C$) in each of the pinning regimes. The consequent predicted values of χ_{ln} and S (calculated with $C=20$) are included also.

Parameter	Single vortex	Small bundle	Large bundle	CDW
n	0	-1/10	7/5	0
m	0	7/10	-3/10	3/2
μ	1/7	5/2	7/9	1/2
χ_{ln}	0	33/50	3/2	3/2
S	0.35	0.02	0.064	0.1

ate. It should be noted that if in some other system, the measurements were to yield field-independent χ_{ln} and S , it would be possible to extract the value of $(n + \mu m)$, but not the individual values of n and m . However for theories predicting $U_{\text{eff}}(J, B, T)$ to be of the form of Eq. (B2) it is questionable whether it is meaningful to consider m and n separately. The validity of doing so would depend on the physical origin of $U_0(B, T)$ and $J_0(B, T)$.

¹G. Blatter, M. V. Feigel'man, V. B. Geshkenbein, A. I. Larkin, and V. M. Vinokur. *Rev. Mod. Phys.* **66**, 4 (1994).

²G. K. Perkins, L. F. Cohen, A. A. Zhukov, and A. D. Caplin. *Phys. Rev. B* **51**, 8513 (1995).

³A. D. Caplin, L. F. Cohen, G. K. Perkins, and A. A. Zhukov. *Supercond. Sci. Technol.* **7**, 412 (1994).

⁴H. G. Schnack, R. Griessen, J. G. Lensink, and Wen Hai-Hu. *Phys. Rev. B* **48**, 13 178 (1993).

⁵M. P. Maley, J. O. Willis, H. Lessure, and M. E. McHenry. *Phys. Rev. B* **42**, 2639 (1990).

⁶M. Däumling, J. M. Seutjens, and D. C. Larbalestier, *Nature (London)* **346**, 332 (1990).

⁷V. V. Moshchalkov, A. A. Zhukov, I. V. Gladyshev, S. N. Gordeev, G. T. Karapetrov, V. D. Kusnetsov, V. V. Metlushko, V. A. Murashov, V. I. Voronkova, and V. K. Janovsky, *J. Magn. Mater.* **90&90**, 611 (1990).

⁸G. K. Perkins *et al.* (unpublished).

⁹A. I. Larkin and Yu. N. Ovchinnikov. *J. Low Temp. Phys.* **34**, 409 (1979).